Journal of Medical Microbiology (2007), **56**, 1536–1548 DOI 10.1099/jmm.0.47289-0

Characterization of RagA and RagB in *Porphyromonas gingivalis*: study using gene-deletion mutants

Keiji Nagano,[1]† Yukitaka Murakami,[1] Kiyoshi Nishikawa,[1] Junpei Sakakibara,[1,2] Kazuo Shimozato[2] and Fuminobu Yoshimura[1]

Correspondence
Yukitaka Murakami
yukimu@dpc.agu.ac.jp

[1]Department of Microbiology, School of Dentistry, Aichi-Gakuin University, 1-100 Kusumoto-cho, Chikusa-ku, Nagoya, Aichi 464-8650, Japan

[2]Oral and Maxillofacial Surgery II, School of Dentistry, Aichi-Gakuin University, 1-100 Kusumoto-cho, Chikusa-ku, Nagoya, Aichi 464-8650, Japan

The major outer-membrane proteins RagA and RagB of *Porphyromonas gingivalis* are considered to form a receptor complex functionally linked to TonB. In this study, *P. gingivalis* mutants with *ragA*, *ragB* or both deleted were constructed from strain W83 as the parent to examine the physiological and pathological functions of RagA and RagB. The double-deletion mutant completely lacked both RagA and RagB, whereas the Δ*ragA* mutant reduced RagB expression considerably and the Δ*ragB* mutant produced degraded RagA. Growth of the three mutants in a nutrient-rich medium and synthetic media containing digested protein as a unique nutrient source was similar to that of the parental strain; however, both the Δ*ragA* and Δ*ragAB* mutants exhibited very slow growth in a synthetic medium containing undigested, native protein, and the two mutants tended to lose their viability during experiments, although gingipain (protease) activities were unchanged in the mutants. A mouse model showed that the Δ*ragB* mutant had reduced virulence. Cell-surface labelling with biotin and dextran revealed that both RagA and RagB localized on the outermost cell surface. A cross-linking experiment using wild-type *P. gingivalis* showed that RagA and RagB were closely associated with each other. Furthermore, co-immunoprecipitation confirmed that RagA and RagB formed a protein–protein complex. These results suggest that physically associated RagA and RagB may stabilize themselves on the cell surface and function as active transporters of large degradation products of protein and in part as a virulence factor.

Received 14 March 2007
Accepted 24 July 2007

INTRODUCTION

Porphyromonas gingivalis, a Gram-negative, asaccharolytic anaerobe, is a major causative agent in the initiation and progression of periodontal disease (Lamont & Jenkinson, 1998). This organism possesses a variety of virulence factors, including fimbriae and haemagglutinins, as well as strong proteolytic enzymes such as Lys- and Arg-gingipains.

The outer membrane of the Gram-negative bacterium directly interacts with other bacteria, host cells and their environment. These interactions must be closely related to growth, colonization, biofilm formation, accomplishment of infection and development of diseases. We have established an isolation method for the outer membrane and identified major outer-membrane proteins designated Pgms 1–7 from *P. gingivalis* strain ATCC 33277^T (hereafter referred to as 33277) (Murakami *et al.*, 2002, 2004). Among the major outer-membrane proteins, Pgm1 and Pgm4 were identified as RagA and RagB, respectively, and their peptide fingerprinting patterns and N-terminal or internal amino acid sequences were compared with those of *P. gingivalis* strain W83, whose complete genome sequence has been published (Nelson *et al.*, 2003). We have also identified major outer-membrane proteins from W83 (Imai *et al.*, 2005). RagA is observed as a 110 kDa protein by SDS-PAGE in both strains, although the mobility of RagB is different, appearing as 47 and 55 kDa proteins in 33277 and W83, respectively.

RagA and RagB were originally identified as immuno-dominant surface antigens recognized by sera from periodontitis patients (Curtis *et al.*, 1991). It has been reported that *ragB*, which is located adjacent to and downstream of *ragA*, is co-transcribed with *ragA* as a

†Present address: Department of Molecular and Cell Biology, University of California, Berkeley, CA 94720-3202, USA.

Abbreviations: CAT, chloramphenicol acetyltransferase; CBB, Coomassie brilliant blue; DAB, 3,3′-diaminobenzidine.

The GenBank/EMBL/DDBJ accession number for the *P. gingivalis* ATCC 33277^T *ragA*, *ragB* and flanking region sequence is AB205195.

polycistronic message, and that expression of *ragAB* is influenced by temperature (Hanley *et al.*, 1999; Bonass *et al.*, 2000). RagA has homology to TonB-linked outer-membrane receptors, which are involved in the recognition and active transport of specific external ligands by a wide range of Gram-negative species (Curtis *et al.*, 1999). RagB is predicted to be a lipoprotein from the primary amino acid sequence and is more diverse than RagA among the species, with only short regions of sequence conservation (Hall *et al.*, 2005; Imai *et al.*, 2005). Based on circumstantial evidence, Hanley *et al.* (1999) claimed that RagA and RagB might form a functionally linked complex on the outer surface of *P. gingivalis*, involved in a TonB-dependent, active process.

Both 33277 and W83 are widely used for *P. gingivalis* studies. 33277 has both long and short fimbriae, encoded by *fimA* and *mfa1*, respectively (Yoshimura *et al.*, 1984; Hamada *et al.*, 1996), whereas W83 lacks both of these, although it possesses apparently intact *fimA* (PG2132, as annotated in the *P. gingivalis* W83 genome database) and *mfa1* (PG0178) disrupted with an insertion element (IS*pg4*). As whole-genome sequencing of 33277 has not yet been carried out, we wanted to analyse the *rag* locus from 33277.

In this study, we determined the DNA sequence of the *ragAB* region from 33277 and compared it with that from W83. Then we constructed three mutants from W83 by deleting the ORFs of *ragA* and/or *ragB*, and examined the physiological and pathological functions of RagA and RagB. We also present experimental evidence that RagA and RagB, localized on the cell surface, are physically and functionally associated with each other.

METHODS

Bacterial strains and growth conditions. The bacterial strains and plasmids used in this study are shown in Table 1 (Gardner *et al.*, 1996; Nelson *et al.*, 2003). All *P. gingivalis* strains were grown at 37 °C under anaerobic conditions [10 % CO_2, 10 % H_2 and 80 % N_2] on *Brucella* HK agar (Kyokuto Pharmaceutical) supplemented with 5 % laked rabbit blood, 2.5 μg haemin ml^{-1}, 5 μg menadione ml^{-1} and 0.1 mg dithiothreitol ml^{-1} (BHK agar), and in trypticase soy broth (Becton, Dickinson) supplemented with 2.5 mg yeast extract ml^{-1}, 2.5 μg haemin ml^{-1}, 5 μg menadione ml^{-1} and 0.1 mg dithiothreitol ml^{-1} (sTSB). For growth experiments, we also used Dulbecco's

Table 1. Bacterial strains and plasmids used in this study

Strain or plasmid	Genotype or relevant characteristics*	Source or reference
Strains		
P. gingivalis		
W83	Parental strain, genome sequenced	Nelson *et al.* (2003)
ATCC 33277^T	Wild-type type strain	ATCC
Δ*ragA*	*ragA*-deletion mutant from W83; Cm^R	This study
Δ*ragB*	*ragB*-deletion mutant from W83; Cm^R	This study
Δ*ragAB*	*ragA* and *ragB*-deletion mutant from W83; Cm^R	This study
Δ*ragB*+$ragB_{W83}$	Δ*ragB* carrying pTCBex2::$ragB_{W83}$	This study
Δ*ragB*+$ragB_{33277}$	Δ*ragB* carrying pTCBex::$ragB_{33277}$	This study
E. coli		
TOP10	Used as chemically competent cells	Invitrogen
S17-1	Used for mobilizing pT-COW to *Bacteroides* and *P. gingivalis* via conjugation	Gardner *et al.* (1996)
Plasmids		
pCR-Blunt II-TOPO	A cloning vector, linearized with DNA topoisomerase I bound to the 3′ end of each DNA strand; Km^R	Invitrogen
pKD260	A derivative of pACYC184 with deletion of a 1.1 kb *Hin*cII fragment, bearing the *cat* gene; Cm^R	A gift from K. Nakayama†
pT-COW	Ap^R and Tc^R in *E. coli*, Tc^R in *Bacteroides* and *P. gingivalis*; Mob^+ Rep^+	Gardner *et al.* (1996)
pTCB	A Tc^R gene-deleted pT-COW; Ap^R in *E. coli*, Tc^R in *P. gingivalis*	This study
pTCBex	A pTCB derivative containing a *fimR* promoter region; Ap^R in *E. coli*, Tc^R in *P. gingivalis*	This study; Nishikawa & Yoshimura (2001)
pTCBex2	A pTCB derivative containing a *rag* promoter region; Ap^R in *E. coli*, Tc^R in *P. gingivalis*	This study
pTCBex::$ragB_{33277}$	A pTCBex derivative containing *ragB* ORF from 33277; Ap^R in *E. coli*, Tc^R in *P. gingivalis*	This study
pTCBex2::$ragB_{W83}$	A pTCBex2 derivative containing *ragB* ORF from W83; Ap^R in *E. coli*, Tc^R in *P. gingivalis*	This study

*Cm^R, chloramphenicol resistance; Tc^R, tetracycline resistance; Ap^R, ampicillin resistance; Km^R, kanamycin resistance.
†Division of Microbiology and Oral Infection, Department of Developmental and Reconstructive Medicine, Nagasaki University Graduate School of Biomedical Sciences.

modified Eagle's medium (DMEM) supplemented with 1 % (w/v) tryptone (Becton, Dickinson), 1 % (w/v) neopeptone (Becton, Dickinson), 1 % (w/v) BSA (fraction V; Miles), or 1 % (w/v) BSA digested with 0.25 % trypsin (Invitrogen) for 10 h at 37 °C. *Escherichia coli* strains were cultivated in Luria–Bertani medium supplemented with the necessary antibiotics. Bacterial growth was monitored by measuring the OD_{660}.

DNA manipulation. Restriction enzymes were purchased from Takara. Plasmid DNA was isolated using a QIAprep Spin Miniprep kit (Qiagen). Genomic DNA was isolated with a Master Pure DNA Purification kit (Epicentre). Standard PCR experiments were performed using a high-fidelity Pyrobest DNA polymerase (Takara) with a PCR Thermal Cycler Dice (Takara). DNA and PCR products were purified with a Freeze 'N Squeeze DNA Gel Extraction kit (Bio-Rad).

DNA sequencing. A purified PCR product and plasmid DNA were usually used as templates for the DNA cycle sequencing with a BigDye Terminator v3.1 Cycle Sequencing kit (Applied Biosystems). The products of the DNA cycle sequencing reaction were purified and analysed using an ABI PRISM 3100-Avant Genetic Analyzer (Applied Biosystems).

ragA, *ragB* and their flanking regions in the 33277 genome were sequenced. We previously examined the N-terminal and several internal amino acid sequences of RagA and RagB of 33277 (Murakami *et al.*, 2002, 2004). Based on these amino acid sequences, primers were designed and the internal region between *ragA* and *ragB* was amplified by PCR and sequenced. Next, the outside sequence of the region was determined by inverse PCR (Ochman *et al.*, 1988). Briefly, the 33277 genome was digested with *Psh*BI and then ligated to generate a pool of monomeric DNA circles. Using the DNA circles as templates, the outside region was amplified by PCR, and the amplified fragment was subjected to DNA sequencing.

Construction of deletion mutants from W83. Deletion mutants were constructed by the PCR-based overlap-extension method (Horton *et al.*, 1993) essentially as described previously (Nagano *et al.*, 2005). The primers and their annealing sites are shown in Table 2 and Fig. 2(a, b), respectively. The *cat* gene, encoding chloramphenicol acetyltransferase (CAT), was amplified with primers AGU01 and AGU02 from pKD260. For construction of the *ragA*-deletion cassette, the flanking sequence upstream of *ragA* was amplified with primers AGU51 and AGU52, which have homology to the 5′ end of the *cat* fragment. The flanking sequence downstream of *ragA* was amplified with AGU56 and AGU55, which have homology to the 3′ end of the *cat* fragment. The *cat*, *ragA*-upstream and *ragA*-downsteam fragments were used as templates for overlap-extension PCR to generate a deletion cassette in which *ragA* was replaced by *cat*. As the inserted *cat* gene contained only its reading frame without a promoter/terminator, its transcription was dependent on the *rag* promoter, and a downstream gene such as *ragB* was expected to be transcribed by the read-through mechanism (Nagano *et al.*, 2005). The deletion cassettes of *ragB* and both *ragA* and *ragB* were generated by similar procedures. Each deletion cassette was ligated into pCR-Blunt II-TOPO (Invitrogen) and the resulting recombinant plasmids were transformed into *E. coli* TOP10 (Invitrogen). A plasmid construct carrying each deletion cassette was sequenced before electroporation to rule out unintended base changes. For electroporation of *P. gingivalis*, the plasmid constructs were linearized by digestion with the endonucleases *Spe*I and *Xba*I, and introduced into electrocompetent cells of W83. After 6 h of anaerobic incubation in sTSB, the pulsed cells were plated on BHK agar supplemented with 10 μg chloramphenicol ml^{-1} and the plates were incubated anaerobically for 7 days.

Complementation of RagB into the *ragB* deletion mutant. The *ragB* deletion mutant (Δ*ragB*) was transformed with the shuttle vector pTCB bearing a DNA fragment that linked the promoter region of *rag*

Table 2. Primers used in this study

Primer-binding sites are shown in Fig. 2. Single underlines show overlapping regions of the 5′ or 3′ end of *cat*. Double underlines indicate restriction enzyme sites.

Name	Sequence (5′→3′)
AGU01*	ATGGAGAAAAAAATCACTGGA
AGU02*	TTACGCCCCGCCCTGCCACTC
AGU51	TTACTGCCACCCCTTTCACTC
AGU52	CCAGTGATTTTTTTCTCCATAGACTTTTCTTTTGCGTTAAA
AGU53	ATTGATGTCCCGATGCCTTATATC
AGU54	CCAGTGATTTTTTTCTCCATATCAAATGTTTCTTAAGAATAAGTAAATCTTAG
AGU55	GCAGGGCGGGGCGTAAGATTTACTTATTCTTAAGAAACATTTG
AGU56	ATCTGCTGCAGCTTTTCCAT
AGU57	GCAGGGCGGGGCGTAATTTAGTTGTAGATCTTACTATGAAATATGG
AGU58	GCACGAACTGGGTTTAGAGC
AGU59	GGGGGGATTTACAACTACTTTC
AGU60	TTATCTGTTTGGTGGATAGGATTATG
fimRPSpeF	TCACTAGTGTGGAAAACATTGGAAAGG
fimRPBamR	ACGGATCCATATTGTGTAATCTTTACGC
ragPNotF	CGAAAAAAATGCGGCCGCCCACTTTATTCCATAAAATCGAACC
ragPBamR	GCGTCATTCTGGATCCAGACTTTTCTTTTGCGTTAAAC
W83ragBBamF	TTAAGAAACAGGATCCATGAAAAAAATAATTTATTGGGTTG
W83ragBHindR	AAGATCTACAAAGCTTTTATATCGGCCAGTTCTTTATTAAC
33277ragBBamF	TTAACAGTAAGGATCCATGAAGAAAATATTTTATGCAGTGC
33277ragBHindR	GAAACATCTAAAGCTTTTAGTTCGGCCAGTTTTTGATAATC

*The same primers were used by Nagano *et al.* (2005).

or *fimR* with the *ragB* ORF from W83 or 33277. To generate restriction sites at the 5′ and 3′ ends of the promoters by PCR, the primers ragPNotF and ragPBamR were used to generate a 482 bp fragment of the *rag* promoter, and fimRPSpeF and fimRPBamR to generate a 460 bp fragment of the *fimR* promoter (Nishikawa & Yoshimura, 2001) (Table 2). The *fimR* and *rag* promoters amplified and digested with appropriate restriction enzymes (*Spe*I/*Bam*HI and *Not*I/*Bam*HI, respectively) were ligated into pTCB digested with the same enzymes to create pTCBex and pTCBex2, respectively (Table 1).

The *ragB* ORF of W83 ($ragB_{W83}$) was amplified with primers W83RagBBamF and W83RagBHindR from the W83 genome. The *ragB* ORF of 33277 ($ragB_{33277}$) was amplified with primers 33277RagBBamF and 33277RagBHindR from the 33277 genome. Amplified $ragB_{W83}$ or $ragB_{33277}$ was digested with *Bam*HI and *Hin*dIII and inserted into pTCBex or pTCBex2 digested with the same enzyme.

The recombinant plasmid vector was introduced into *E. coli* S17-1 by electroporation. We confirmed that the DNA sequence of the insert had no unintentional base changes after extraction of the plasmid from the transformants. The purified plasmid was then introduced into Δ*ragB* via conjugation under aerobic mating conditions at 37 °C for 12 h and the mated bacteria were spread on BHK agar containing 100 μg gentamicin ml^{-1} and 1 μg tetracycline ml^{-1} (Nishikawa & Yoshimura, 2001). After the plates had been incubated anaerobically for about 1 week at 37 °C, the plasmid was extracted again from black-pigmented transformants and verified by PCR and restriction enzyme digestion analysis.

Cell fractionation, SDS-PAGE and Western blotting. Preparation of the bacterial whole-cell lysate and envelope fraction, SDS-PAGE and Western blotting analyses were performed essentially as described previously (Murakami *et al.*, 2002; Nagano *et al.*, 2005). For co-immunoprecipitation, whole-cell lysate was prepared using BugBuster HT protein extraction reagent according to the manufacturer's instructions (Novagen). The gels were stained with Coomassie brilliant blue R-250 (CBB). As primary antibodies in Western blotting, we used antigen-specific antisera against RagA and RagB obtained from a rabbit immunized with purified RagA protein from 33277 (Murakami *et al.*, 2004) and recombinant RagB constructed on the basis of the W83 sequence (Imai *et al.*, 2005), respectively.

Animal experiments. *P. gingivalis* strains were grown in sTSB for 24 h until the early stationary phase, harvested and washed twice with 10 mM PBS (pH 7.4). The bacterial concentration (c.f.u. ml^{-1}) was adjusted with PBS by reference to a standard curve of concentration against OD_{660}. The numbers of viable cells prepared were counted and confirmed by spreading the bacterial suspension on BHK agar for every experiment. Six-week-old BALB/c mice were challenged with a dorsal subcutaneous injection of 0.2 ml of bacterial suspension. General health, weight and the appearance and location of lesions were assessed daily. To determine bacteraemia, spleens were excised under aseptic conditions, placed in sTSB, minced and suspended gently by pipetting. Different dilutions of these suspensions were spread on BHK agar and cultured anaerobically for 1 week. Black colonies, which are characteristic of *P. gingivalis*, were counted. Only a few colonies without black pigmentation were observed. The black colonies randomly selected were confirmed as *P. gingivalis* by microscopic examinations such as Gram staining. Statistical analyses were performed using Student's *t*-test. Values that were significantly different from control values ($P < 0.05$) are indicated by asterisks in the figures. These animal experiments were performed in accordance with the Guidelines for Animal Experiments at the School of Dentistry, Aichi-Gakuin University.

Antimicrobial susceptibility. The antibiotics used were ampicillin (Wako Pure Chemical Industries), cefotaxime, cefuroxime, cephalexin, ceftriaxone, chloramphenicol, erythromycin, tetracycline, minocycline and norfloxacin (Sigma-Aldrich). MICs were evaluated by an agar double-dilution assay, as recommended by the NCCLS (1997). Briefly, serial dilutions of the corresponding antibiotics were added to BHK agar. After the bacteria had been grown to the early stationary phase in sTSB, 2 μl bacterial culture was spotted on the antibiotic-containing agar. After 2 days of anaerobic incubation, the susceptibility breakpoints were determined.

Electron microscopy. *P. gingivalis* cells were grown to the early stationary phase in sTSB and directly spotted onto carbon-coated grids. After negative staining with 2 % (w/v) uranyl acetate, the cells were observed using a JEM-1210 electron microscope (JEOL).

Cell-surface labelling. *P. gingivalis* cells suspended in 10 mM PBS (pH 8.0) were labelled with sulfo-NHS-LC-biotin (Pierce) at 4 °C for 2 h. The reaction was stopped by the addition of 0.1 M glycine. Dextran labelling was carried out by the method of Kamio & Nikaido (1977). Briefly, Dextran T-10 (Pharmacia) activated with CNBr was added to *P. gingivalis* cells suspended in 0.1 M sodium carbonate buffer (pH 8.5). Coupling was carried out at 20 °C for 1 h and terminated by the addition of 1 M ethanolamine/HCl (pH 7.4). After labelling, envelope fractions were subjected to SDS-PAGE and blotted onto nitrocellulose membranes. Biotinylation was detected using peroxidase-conjugated streptavidin using 3,3′-diaminobenzidine (DAB). Dextran-labelled proteins were detected by Western blotting using anti-RagA and anti-RagB antibodies developed with a Pro-Q Western blot stain kit (Invitrogen).

Chemical cross-linking. Washed *P. gingivalis* cells were suspended in 0.1 M triethanolamine/HCl buffer (pH 8.5). The cross-linker disuccinimidyl suberate (11 Å length; Sigma-Aldrich) dissolved in DMSO was added to a final concentration of 50 mM. After incubation of the reaction mixture at 4 °C for 2 h, the cross-linking reaction was stopped by the addition of 0.1 M Tris/HCl buffer (pH 8.0). The envelope fraction was prepared from the cells and analysed by SDS-PAGE and Western blotting using anti-RagA and anti-RagB antibodies developed with DAB.

Co-immunoprecipitation. Co-immunoprecipitation was performed using a ProFound Co-Immunoprecipitation kit (Pierce) according to the manufacturer's instructions. Briefly, an anti-RagA or anti-RagB antibody was coupled to AminoLink Plus Gel. The slurry of antibody-coupled beads was incubated with whole-cell lysate from W83 with gentle rocking overnight at 4 °C. Beads were washed three times with Dulbecco's PBS. The bound proteins were eluted from the beads with ImmunoPure IgG Elution Buffer, immediately neutralized with 1 M Tris/HCl (pH 9.5) and analysed by SDS-PAGE.

RESULTS AND DISCUSSION

Comparison of RagA and RagB in W83 and 33277

ragA, *ragB* and their flanking regions in 33277 were sequenced. The amino acid sequences deduced from the nucleotide sequences of W83 and 33277 were aligned using CLUSTAL W (Thompson *et al.*, 1994) as shown in Fig. 1. For RagA, a sequence identity of 70 % and a sequence similarity of 81 % were found between the two strains, and the N- and C-terminal domains were almost identical. The regions boxed in RagA in Fig. 1 are conserved in TonB-linked proteins (Hanley *et al.*, 1999). These regions were completely or highly conserved between the strains. In contrast, RagB in W83 and 33277 showed only 48 % identity and 63 % similarity over the whole region. When

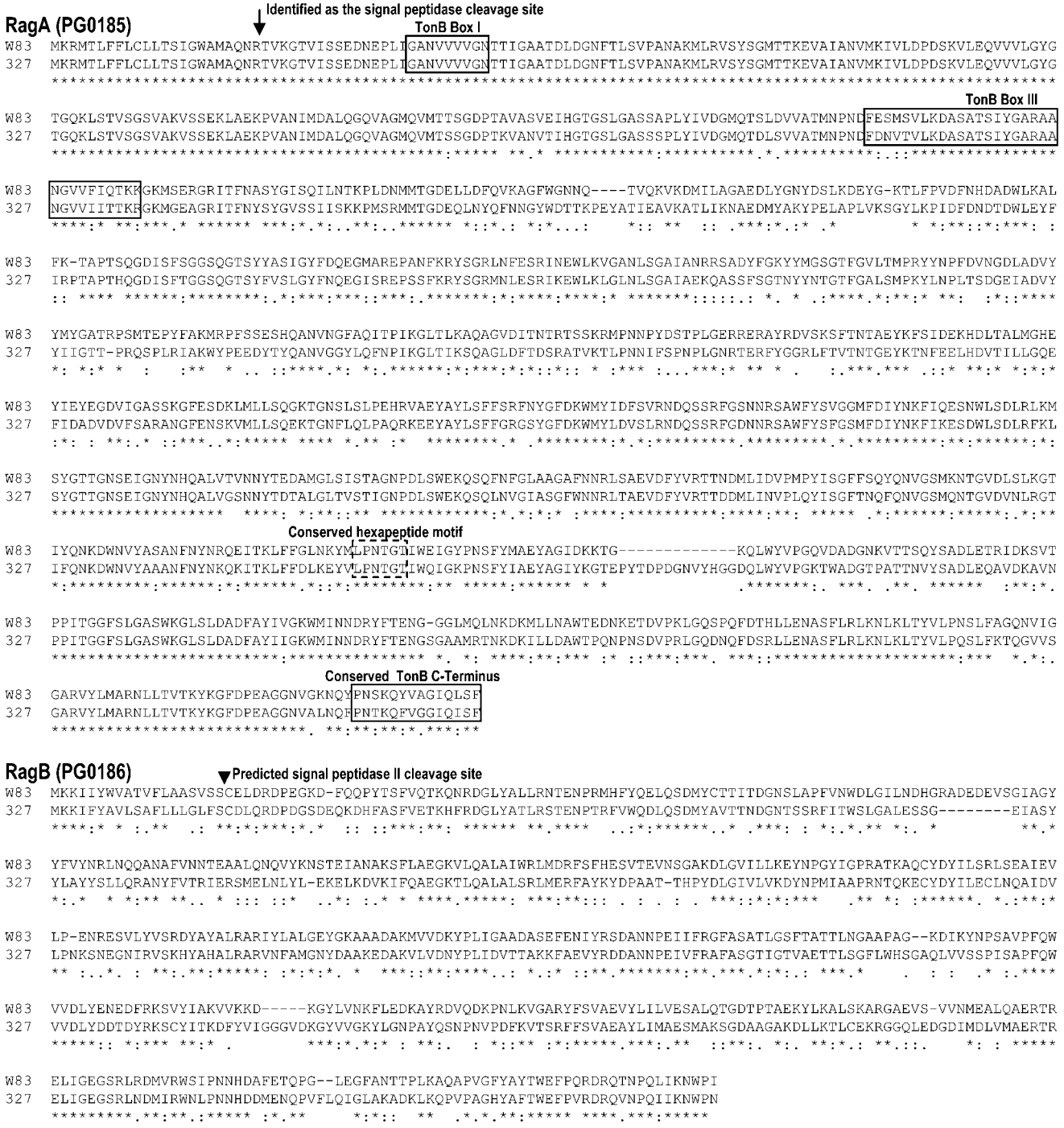

Fig. 1. Alignment of the RagA and RagB sequences of *P. gingivalis* W83 (W83) and ATCC 33277^T (327) by CLUSTAL W. In RagA, TonB boxes and the conserved TonB C-terminus are shown in boxes, and the conserved hexapeptide motif involved in membrane anchoring is shown in a dashed box. The arrow in RagA indicates the signal peptidase cleavage site located at the threonine residue as the N-terminus, identified by the N-terminal sequence (Murakami *et al.*, 2002). The arrowhead in RagB indicates the predicted signal peptidase II cleavage site at the cysteine residue as the N-terminus. Asterisks, two dots and one dot indicate identical, strongly conserved and weakly conserved residues, respectively, between the two sequences of the strains.

the nucleotide sequences of W83 and 33277 were also compared, *ragA* showed a higher sequence identity (72 %) than *ragB* (59 %). The *ragB* locus including *ragA* was found only in 17 of the 132 *P. gingivalis* strains by Southern blot analysis using a DNA probe (436 bp) derived from *P. gingivalis* strain W50 and was present mostly in virulent

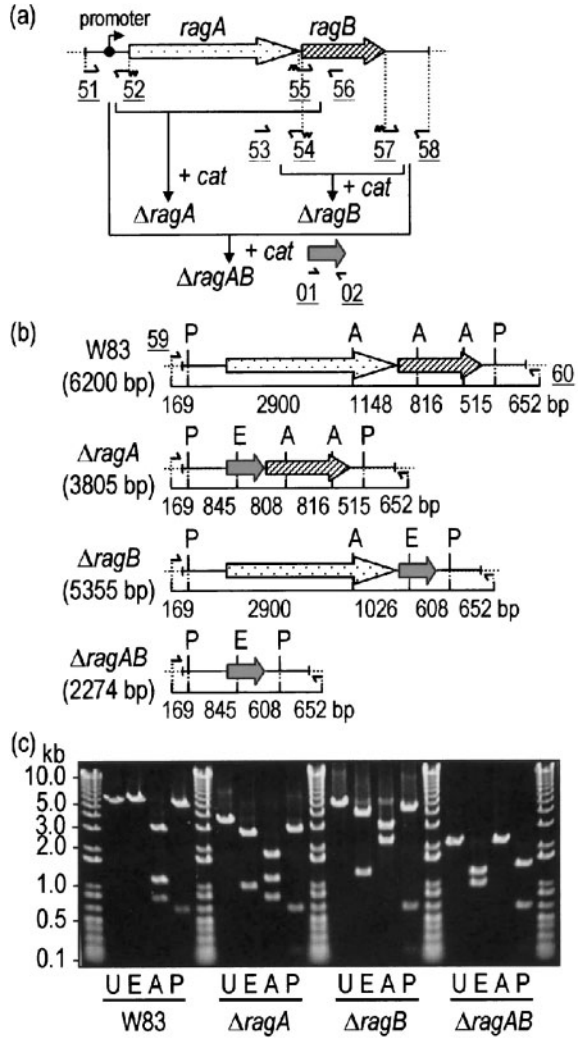

Fig. 2. Construction of *ragA* and *ragB* deletion mutants from *P. gingivalis* W83. (a) Gene arrangement in the chromosome, procedure for construction of allele-exchange gene-deletion and the location of primers. (b) Restriction sites and predicted lengths of the DNA regions in each genotype. The sizes (bp) of the DNA regions are indicated. (c) Verification of the mutants by gel electrophoresis of PCR products. After amplification by PCR with primers AGU59 and AGU60 shown at the top of (b) as 59 and 60, respectively, the PCR products were digested with restriction enzymes described below and subjected to electrophoresis. *ragA*, dotted arrows; *ragB*, diagonal-line arrows; *cat*, shaded arrows; primers, small arrows; overlap regions on *cat*, wavy lines. Underlined numbers indicate simplified primer designation (see Table 2 for details). U, Undigested; E, digested with *Eco*RI; A, digested with *Acc*I; P, digested with *Psh*BI. DNA size marker bands are indicated (kb).

strains, but not in 381 and 33277 (Hanley *et al.*, 1999; Frandsen *et al.*, 2001). However, we have reported that 33277 expresses both RagA and RagB in the outer membrane, based on peptide mapping and internal sequence analysis (Murakami *et al.*, 2002, 2004) and Western immunoblotting (Imai *et al.*, 2005). In this study, we verified by sequencing that the genes *ragA* and *ragB* were present in the 33277 chromosome. More recently, Hall *et al.* (2005) reported sequence diversity and antigenic variation at the *rag* locus, which was classified into four alleles. The *rag* locus was in the same genomic location; however, there was some polymorphism. W83 and 33277 represented *rag-1* and *rag-4*, respectively, in the report. The *ragAB* nucleotide sequence from 33277 in our study (GenBank accession no. AB205195) was identical to that derived by Hall *et al.* (2005) (GenBank accession no. AY842852). The degree of similarity between RagB variants (43–56 % identity at the protein level and 53–62 % identity at the nucleotide level) would not have been detected by Southern blotting under high-stringency conditions (Frandsen *et al.*, 2001).

Construction of deletion mutants

Three deletion mutants from W83 were constructed. In these ORFs, *ragA* and/or *ragB* were deleted and replaced by *cat* using the PCR-based overlap-extension method. The overall design for construction of the mutants is shown in Fig. 2(a). To confirm the replacement of target ORFs by *cat*, the cloning sites were amplified from flanking regions by PCR using each mutant chromosome as a template with primers of AGU59 and AGU60 designed to anneal outside the cloning sites as shown in Fig. 2(b). Amplified PCR products were then digested with selected restriction enzymes to verify the genotypes of the putative mutants. As shown in Fig. 2(c), gel electrophoresis of digested DNA yielded the predicted fragments. Thus three mutants of W83 with deletion of *ragA* (Δ*ragA*), *ragB* (Δ*ragB*) or both (Δ*ragAB*) were obtained.

Complementation of RagB

Complementation analysis was performed with shuttle plasmid pT-COW derivatives incorporating the *ragA* and *fimR* promoters, presumed to be strong and weak promoters, respectively (Gardner *et al.*, 1996; Nishikawa & Yoshimura, 2001). Although we tried to construct a series of Δ*ragB* complemented with *ragB*, namely *ragB* from W83 ($ragB_{W83}$) or *ragB* from 33277 ($ragB_{33277}$) under the *rag* promoter and $ragB_{W83}$ or $ragB_{33277}$ under the *fimR* promoter, we obtained only two strains: $ragB_{W83}$ downstream of the *rag* promoter (Δ*ragB*+$ragB_{W83}$) and $ragB_{33277}$ downstream of the *fimR* promoter (Δ*ragB* +$ragB_{33277}$) (Table 1). Although further research is required to determine the reason for this, various explanations include the possibility that: (i) $RagB_{33277}$ may not be compatible with $RagB_{W83}$ because of their low homology (Hall *et al.*, 2005); and (ii) full expression of $RagB_{33277}$ via the *rag* (strong and authentic) promoter in Δ*ragB* in the presence of $RagA_{W83}$ may cause cell viability to deteriorate, resulting in failure to establish the complementation strain carrying pTCBex2::$ragB_{33277}$. Also, insufficient expression of $RagB_{W83}$ via the *fimR*

(weak) promoter may make cells unstable in the presence of sufficient $RagA_{W83}$ in Δ*ragB* as shown in the following section. We did not attempt to complement *ragA* into Δ*ragA* because of the lower viability during experiments with the mutant (see section on physical and morphological characteristics later).

SDS-PAGE and Western blot analyses of envelope fractions

Envelope fractions denatured in SDS with 2-mercaptoethanol were subjected to SDS-PAGE and visualized with CBB (Fig. 3a). The 110 kDa band of RagA was clearly observed at high intensity in 33277 and W83, and at low intensity in Δ*ragB*, whereas such bands were not observed in Δ*ragA* or Δ*ragAB*. Complemented Δ*ragB*+$ragB_{w83}$ was able to recover the 110 kDa band (RagA) with higher intensity than Δ*ragB*, whereas RagA was recovered in Δ*ragB* +$ragB_{33277}$ at a low level similar to Δ*ragB*. RagB bands of high intensity were clearly observed at 47 and 55 kDa in 33277 and W83, respectively, and with low intensity in Δ*ragB*+$ragB_{w83}$; however, corresponding bands were not observed in the other strains, Δ*ragA*, Δ*ragB*, Δ*ragAB* and Δ*ragB*+$ragB_{33277}$. RagA and RagB could be detected on SDS-PAGE gels even in whole-cell lysates, although their contents were higher in the envelope fraction, indicating that the proteins in the mutants localized on the membrane as in the parent.

To verify these assignments, envelope fractions separated by SDS-PAGE were subjected to Western blot analyses with antigen-specific antisera against RagA (Fig. 3b) and RagB (Fig. 3c). The anti-RagA antibody detected a strong band of 110 kDa in 33277 and W83 and several weaker bands of lower molecular masses, which appeared to be degradation products. In Δ*ragB*, a new strong 60 kDa band was detected, although a weak signal was seen at the 110 kDa position. Such bands were not observed in Δ*ragA* or Δ*ragAB*. Δ*ragB*+$ragB_{w83}$ was able to recover a strong 110 kDa band together with several lower-molecular-mass bands, including a faint 60 kDa band, although overall signals appeared to be slightly weaker than those of W83. In contrast, in Δ*ragB*+$ragB_{33277}$, the signal intensity of RagA did not increase; the 110 kDa band and several other bands were not recovered to the level of Δ*ragB*+$ragB_{w83}$. The anti-RagB antibody detected weak and strong signals in 33277 (47 kDa) and W83 (55 kDa), respectively. As antiserum against the RagB antigen from W83 was used, the signal for RagB from 33277 was weak, indicating an antigenic difference between the two strains (note the two equivalent CBB-stained RagB bands of lanes 1 and 2 in Fig. 3a compared with the two clearly different immunostained bands in the same lanes in Fig. 3c). The migration position of RagB following SDS-PAGE was also clearly different between the two strains. The precise reason is unclear; however, we speculate that the degree of lipid modification might be different in lipoprotein RagB, as the

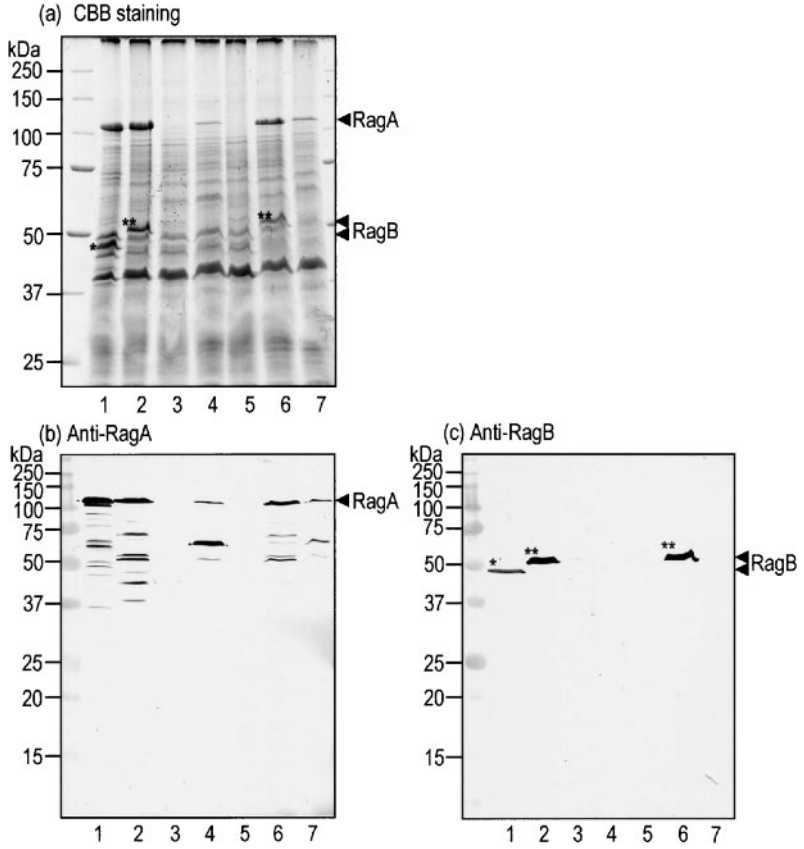

Fig. 3. Protein patterns following SDS-PAGE and Western blotting of envelope fractions. SDS-PAGE gels were stained with CBB (a) and subjected to Western blot analysis with anti-RagA (b) and anti-RagB (c) sera using the chromogenic substrate 4-chloro-1-naphthol. Lanes: 1, 33277; 2, W83; 3, Δ*ragA*; 4, Δ*ragB*; 5, Δ*ragAB*; 6, Δ*ragB* complemented with *ragB* from W83; 7, Δ*ragB* complemented with *ragB* from 33277. Asterisks and double asterisks indicate RagB from 33277 and W83, respectively.

calculated molecular mass and isoelectric point were almost the same in the two strains. When the protein motif was analysed by the Motif Scan program (http://myhits.isb-sib.ch/cgi-bin/motif_scan), nine possible *N*-myristoylation sites were detected in 33277, whereas there were four sites in W83. RagB was not detected in Δ*ragB* and Δ*ragAB*, whereas a faint band was detected in Δ*ragA*. The marked decrease in RagB may not be a polar effect in Δ*ragA* as the inserted *cat* gene was supposed to be a non-polar cassette. Instead, the decrease in RagB may have been caused by a deficiency in RagA due to instability of RagB alone in the outer membrane as discussed later.

As production of RagA was decreased by deletion of RagB as described above, both RagA and RagB may exist as mutually associated structures, and their interaction is probably important in their stabilization in cells. Expression of RagA and RagB in Δ*ragB*+$ragB_{w83}$ was almost fully recovered and the degradation product of RagA (60 kDa protein) disappeared. In contrast, recovery of RagA and RagB in Δ*ragB*+$ragB_{33277}$ was marginal, although the 60 kDa protein derived from RagA decreased and $RagB_{33277}$ was not detected, partially due to the use of an antiserum with less specificity for $RagB_{33277}$. This also suggested that $RagB_{33277}$ under the *fimR* promoter was not expressed sufficiently and might not interact with $RagA_{W83}$ adequately because of their incompatibility.

Physical and morphological characteristics

Δ*ragA* and Δ*ragAB* tended to lose their viability during experiments. We therefore investigated whether they became more oxygen sensitive than the parental strain W83. However, we did not observe any difference in oxygen sensitivity between them (data not shown). These mutants probably had decreased resistance to physical stresses such as centrifugal force, mixing and pipetting. It is possible that the complete disappearance of RagA existing on the outer membrane in large amounts might destabilize the membrane and make it fragile. Such fragility was not observed in Δ*ragB*, presumably due to the presence of RagA to some degree. We did not observe any morphological changes in the three mutants when they were compared with W83 by negative staining in electron microscopy (data not shown).

Growth in nutrient-rich and synthetic media

An early stationary-phase culture in sTSB, a nutrient-rich medium, was inoculated at a 1 : 20 ratio into several media. In sTSB (Fig. 4a), the three mutants Δ*ragA*, Δ*ragB* and Δ*ragAB* showed growth rates similar to the parental strain W83 and reached the stationary phase within 24 h. The three mutants also showed growth curves similar to the parental strain in DMEM supplemented with 1 % tryptone (Fig. 4b) and 1 % neopeptone (data not shown). In DMEM supplemented with 1 % BSA, the parental strain reached the stationary phase within 36 h, slightly later than in sTSB, and Δ*ragB* reached it even later, whereas Δ*ragA* and Δ*ragAB* grew considerably slower and reached the same level as the parental strain at about 72 h (Fig. 4c). However, in DMEM supplemented with BSA pre-digested with trypsin, Δ*ragA* and Δ*ragAB* showed growth curves similar to the parental strain and Δ*ragB* (Fig. 4d). It has been reported that *P. gingivalis* utilizes proteins such as serum albumin as nutrition by digestion with gingipains (Grenier *et al.*, 2001). The amounts and activities of gingipains were almost the same among the strains used here (data not shown). Therefore, the mutants, especially

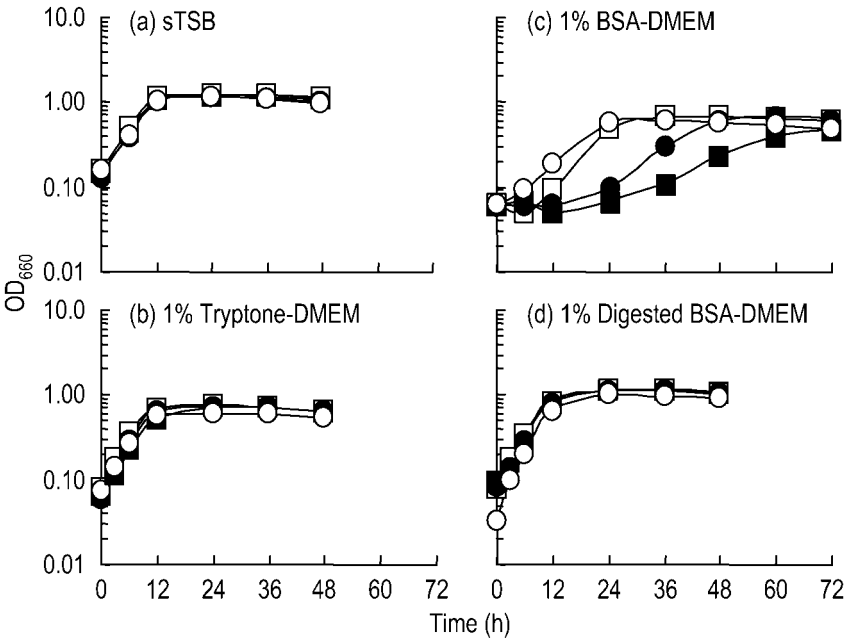

Fig. 4. Growth curves in various media. An early-stationary-phase culture in sTSB was inoculated at a 1 : 20 ratio into sTSB (a) or into DMEM supplemented with 1 % tryptone (b), 1 % BSA (c) or 1 % pre-digested BSA (d). Growth experiments were repeated at least twice and typical results are shown. ○, *P. gingivalis* W83 (parental strain); ●, Δ*ragA*; □, Δ*ragB*; ■, Δ*ragAB*.

Δ*ragA* and Δ*ragAB*, deficient in RagA and RagB, might not uptake larger peptides and thus would need more time to grow until smaller peptides become available via further digestion of BSA with the many proteases in this organism. Digestion of BSA by trypsin or tryptone, a pancreatic digest of casein, could diminish such growth lags, resulting in no apparent difference in growth curves. RagAB could play a role in the active transport of macromolecules such as larger peptides that are not passively permeable to the outer membrane in this organism. This is the first experimental evidence that this assumption is likely, although RagAB has been suggested to play a role in the uptake of macromolecules such as polysaccharides or glycoproteins based on sequence comparison with *Bacteroides thetaiotaomicron* SusCD (Curtis *et al.*, 1999; Hall *et al.*, 2005). However, further work is required to elucidate the exact function of RagAB.

Animal experiments

It has been reported that injection of *P. gingivalis* cells results in necrotizing ulcer formation in the abdomen (Kumagai *et al.*, 2000). Although *P. gingivalis* inhabits periodontal tissue, this experimental model is often used to evaluate pathogenicity.

Bacterial cells of W83 (2×10^9 or 1×10^9 c.f.u.) or Δ*ragB* (4×10^9 or 2×10^9 c.f.u.) were injected into five mice each. Δ*ragA* and Δ*ragAB* were not used in animal experiments because they tended to lose their viability during the experimental procedure, as described above. One day after injection, ruffled hair was observed in every mouse. Although body weight fell from 2 to 4 days after injection, it then recovered and began to increase again. All of the animals injected survived for the experimental period of 2 weeks because the cell numbers used were much lower than those used by others (Kumagai *et al.*, 2000). Abdominal ulcers were observed within 2 days in all mice injected with 2×10^9 c.f.u. W83 and in two mice injected with 1×10^9 c.f.u W83. Ulcer formation was also observed in all mice within 2 days when 4×10^9 c.f.u. Δ*ragB* was injected; however, ulcer size was clearly smaller than that induced by 2×10^9 c.f.u. W83. Only small ulcers were formed in three mice after injection of 2×10^9 c.f.u. Δ*ragB*. These results suggested that Δ*ragB* might be less virulent than the parental W83.

To examine the difference in virulence between the strains quantitatively, bacterial cell numbers in the spleen were also evaluated. As a pilot study, 1×10^9 c.f.u. W83 was injected and bacterial cells in the spleen were counted in three mice every day from days 1 to 7. *P. gingivalis* was detected in all three mice at day 1 and in two of the three mice at day 2. At days 3 to 5, a small number of *P. gingivalis* cells were detected in a mouse with a large lesion. However, at days 6 and 7, *P. gingivalis* was not detected in any mouse. *P. gingivalis* was not detected in mice injected only with PBS as a control. Therefore, we decided to inject 1×10^9 c.f.u. W83, Δ*ragB* or Δ*ragB*+*ragB*$_{W83}$ to count bacterial cell numbers in the spleen at days 1 and 2. At days 1 and 2, 10^4–10^7 c.f.u. W83 per spleen was detected in all four mice. In contrast, much lower cell numbers were detected in two mice and one mouse out of four at days 1 and 2, respectively, and almost no bacteria were detected in five other mice in the case of Δ*ragB* (Fig. 5). Unexpectedly, bacteria were not detected when the complementation strain Δ*ragB*+*ragB*$_{W83}$ was used. We do not know the exact reasons for this, but there are at least two possible explanations. First, although RagB almost recovered to the normal level, RagA was not fully stabilized, as shown in Fig. 3. Secondly, the strain, bearing a recombinant plasmid vector with a large size, might become weak *in vivo*.

It had been considered that RagB or the *rag* locus is related to virulence, as they are frequently detected in *P. gingivalis* strains isolated from deep periodontal pockets (Curtis *et al.*, 1999; Hanley *et al.*, 1999). However, we have recently reported that both RagA and RagB are widely expressed in various strains, including 33277, which has been considered a non-virulent strain, although RagB has several variations (Imai *et al.*, 2005). The relationship between RagB and periodontal disease is unclear, as a proper animal model for periodontal disease has not yet been developed. However, we showed that RagB deletion reduced virulence in mice, suggesting that RagA and RagB are functionally related to survival, growth and expression of virulence of *P. gingivalis in vivo* directly or indirectly. Very recently, Shi *et al.* (2007) reported that both RagA and RagB mutants are less virulent than the wild-type in a similar murine model.

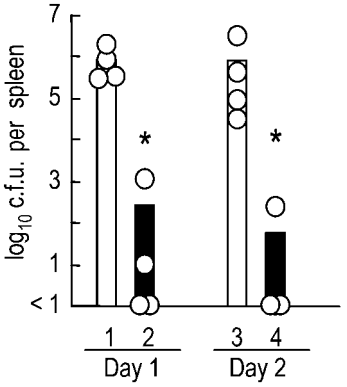

Fig. 5. Viable cell numbers of *P. gingivalis* in spleens of mice inoculated with 1×10^9 c.f.u. W83 (lanes 1 and 3, open columns) or Δ*ragB* (lanes 2 and 4, closed columns). Spleens were excised at 1 (lanes 1 and 2) and 2 (lanes 3 and 4) days after inoculation and spread on BHK agar after homogenization in sTSB broth. After anaerobic culture, black colonies that appeared were counted as *P. gingivalis*. Circles and columns indicate values of individuals and means, respectively. Significant differences between the two groups ($P<0.05$) as determined by Student's *t*-test are indicated by asterisks.

Antimicrobial susceptibility and other characteristics

We also examined whether deletion of RagA and/or RagB influenced MICs to various antibiotics. The MIC of chloramphenicol for the wild-type was 4 μg ml^{-1}, whilst for the mutants it was 64 μg ml^{-1}, presumably due to the strong CAT expression. Strong CAT activity was detected only in mutants where *cat* had been introduced (data not shown). However, no significant difference in the MICs of other antibiotics was observed between the wild-type and mutants. Moreover, the various antibiotics used were effective against the *P. gingivalis* strains, showing considerably low MICs. It has been reported that *P. gingivalis* is susceptible to most antibiotics, including β-lactams, partially due to the absence of β-lactamase (Andrés *et al.*, 1998; Kleinfelder *et al.*, 1999; Ikeda & Yoshimura, 2002). Thus we concluded that RagA and RagB might not be involved in antimicrobial susceptibility.

In addition, we tested the effects of deletion of RagA and/or RagB on haemagglutinating activity as one of the representative characteristics of *P. gingivalis*; however, no difference from the parental strain was observed, implying that they were unrelated to this characteristic (data not shown).

Cell-surface labelling

To examine localization of RagA and RagB, we used different labelling molecules, namely biotin and dextran. Both RagA and RagB were strongly detected by a streptavidin-linked reagent after biotinylation (Fig. 6b), based on comparison with patterns after amido black staining (Fig. 6a). Sulfo-NHS-LC-biotin has been demonstrated predominantly to label cell-surface proteins of Gram-negative bacterial cells (Bradburne *et al.*, 1993). However, as this reagent is relatively small (M_r 557) and hydrophilic, it may penetrate the outer membrane through diffusion pores such as porins, and outer-membrane proteins might be labelled from the periplasmic space. Therefore, we used macromolecular dextran as another labelling reagent that could not pass through the outer-membrane pores. After CNBr-activated dextran labelling, the intensities of RagA and RagB bands decreased, whereas thick smears appeared at the top of the separation gel (Fig. 7a), indicating that RagA and RagB were shifted up by conjugation with dextran. Western blotting using anti-RagA and anti-RagB antibodies confirmed that large quantities of both RagA and RagB existed in the high-molecular-mass smears after labelling (Fig. 7b, c). Consequently, these results suggested that both RagA and RagB were exposed on the cell surface.

Chemical cross-linking

After chemical cross-linking, both RagA and RagB bands at the appropriate positions almost disappeared; instead, heavily stained, diffuse bands appeared as high molecular masses of more than 200 kDa in CBB-stained gels (Fig. 8a). Western blotting using specific antibodies confirmed that most RagB migrated to much higher positions as high-molecular-mass bands, although RagA behaved in a slightly different manner (Fig. 8b, c). These results suggested that RagA and RagB were in close proximity and physically interacted with each other.

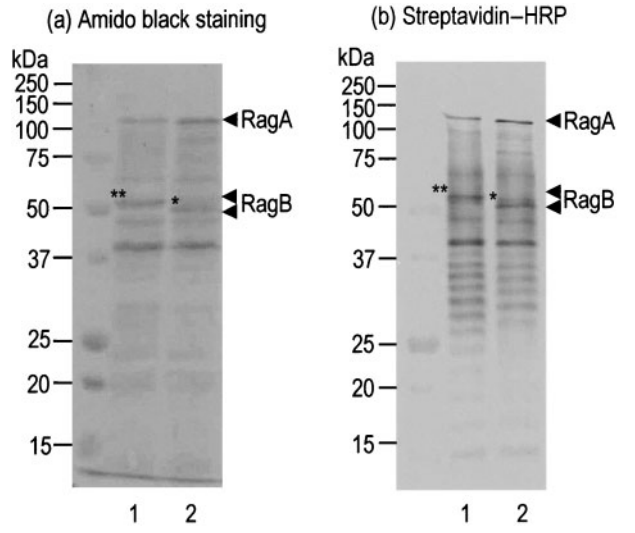

Fig. 6. Cell-surface labelling with biotin. *P. gingivalis* cells were labelled with sulfo-NHS-LC-biotin at 4 °C for 2 h. Envelope fractions from the labelled cells were subjected to SDS-PAGE and then transferred onto nitrocellulose membranes. Proteins were stained with amido black (a), and biotinylated molecules were detected with streptavidin–horseradish peroxidase (HRP) (b). Lanes: 1, W83; 2, 33277. Asterisks and double asterisks indicate RagB from 33277 and W83, respectively.

Co-immunoprecipitation

The anti-RagA antibody precipitated RagA and RagB proteins, and the anti-RagB antibody also precipitated both proteins (Fig. 9). Essentially, no other bands were stained. This strongly suggested that RagA and RagB have a physical molecular interaction that permits them to be chemically cross-linked as described above.

Conclusions

This is the first report on RagA and RagB characterized using deletion mutants. We have demonstrated that both *ragA* and *ragB*, tandemly arranged in this order, are required for stable expression of RagA and RagB. When *ragA* was deleted, RagB was expressed only at a negligible level. Deletion of *ragB* led to RagA degradation. We also showed that deletion mutants had retarded bacterial growth in a nutrient-poor synthetic medium and had decreased infective activity. Chemical cross-linking and

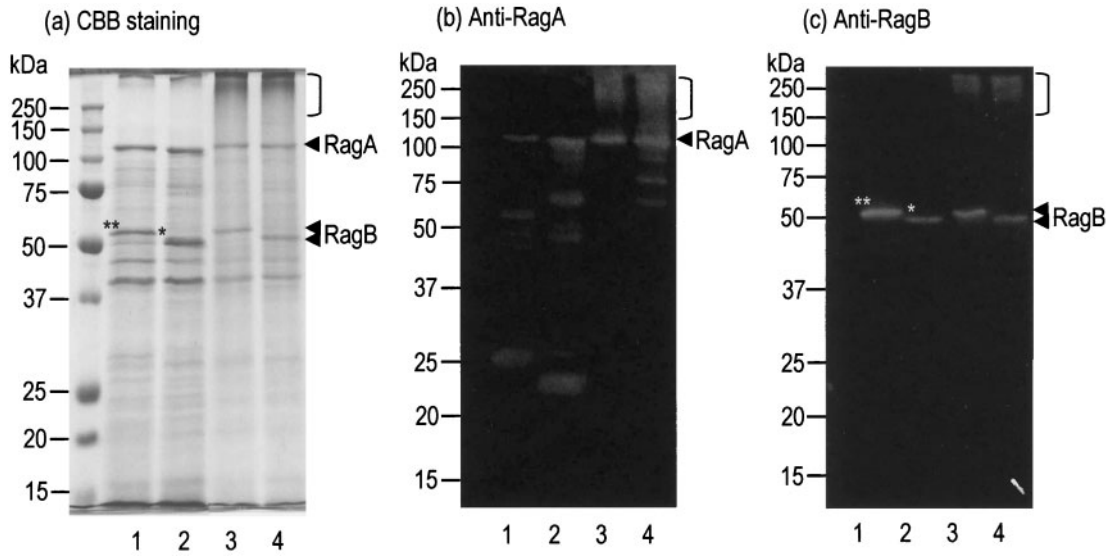

Fig. 7. Cell-surface labelling with activated dextran. *P. gingivalis* cells were labelled with CNBr-activated dextran T-10 at 20 °C for 1 h. The envelope fraction was prepared from the labelled cells and analysed by SDS-PAGE. The gels were stained with CBB (a) and subjected to Western blot analysis with anti-RagA (b) and anti-RagB (c) sera using a Pro-Q Western blot stain kit. Lanes: 1, unlabelled W83; 2, unlabelled 33277; 3, labelled W83; 4, labelled 33277. Asterisks and double asterisks indicate RagB from 33277 and W83, respectively. Brackets indicate dextran–protein complexes as smears.

co-immunoprecipitation experiments revealed a physical, molecular association of RagA and RagB. Both RagA and RagB were identified as proteins exposed on the cell surface after labelling experiments. In conclusion, RagA and RagB, which stabilize each other, may form functionally associated complexes in the outer membrane of *P. gingivalis*.

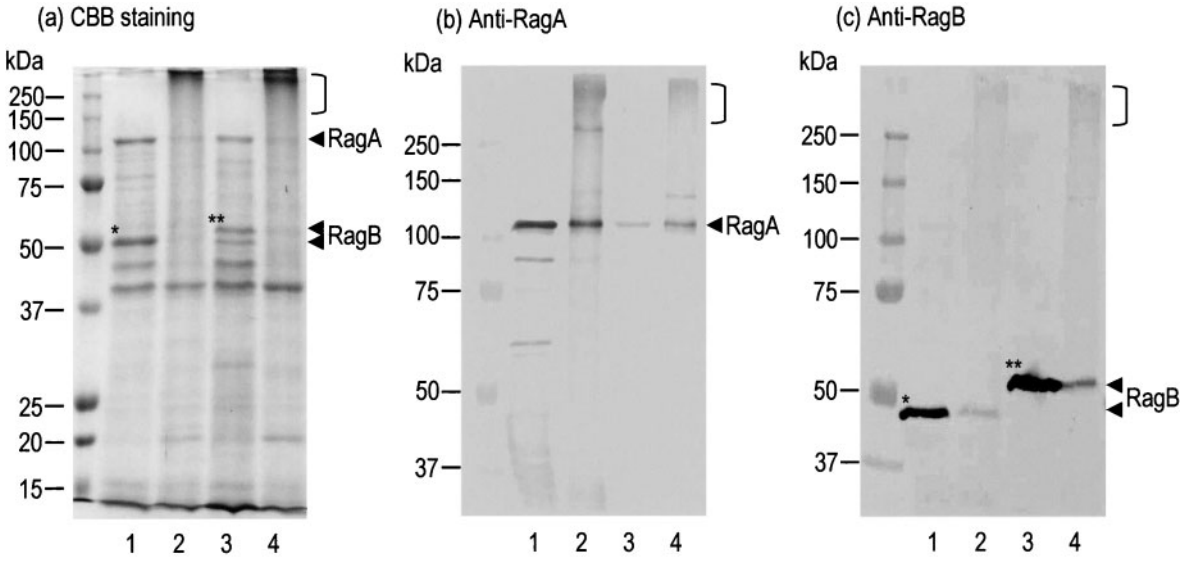

Fig. 8. Chemical cross-linking of *P. gingivalis* wild-type RagA and RagB. Bacterial cells were treated with disuccinimidyl suberate as a cross-linker at 4 °C for 1 h. Envelope fractions from the cross-linked cells were analysed by SDS-PAGE. The gels were stained with CBB (a) and subjected to Western blot analysis with anti-RagA (b) and anti-RagB (c) sera using the chromogenic substrate DAB. The RagA band in lane 3 of (b) was not detected adequately in this case. Lanes: 1, uncross-linked 33277; 2, cross-linked 33277; 3, uncross-linked W83; 4, cross-linked W83. Asterisks and double asterisks indicate RagB from 33277 and W83, respectively. Brackets indicate cross-linked proteins as smears.

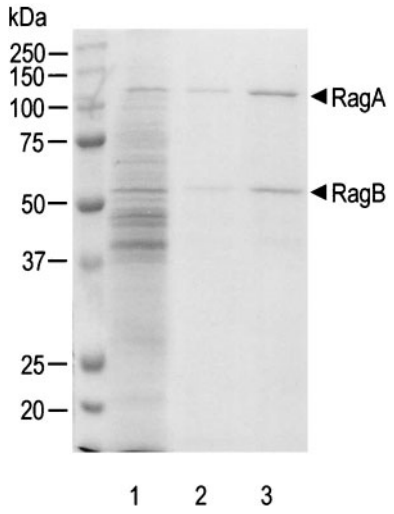

Fig. 9. Co-immunoprecipitation of *P. gingivalis* W83 whole-cell lysate with anti-RagA and RagB antibodies. Co-immunoprecipitation was performed using a ProFound Co-Immunoprecipitation kit. Whole-cell lysate prepared with BugBuster HT protein extraction reagent was added to AminoLink Plus Gel coupled with an anti-RagA or anti-RagB antibody. After gentle rocking overnight at 4 °C, the beads were washed three times with Dulbecco's PBS. Bound proteins were eluted with ImmunoPure IgG Elution Buffer and analysed by SDS-PAGE. The gel was stained with CBB. Lanes: 1, W83 whole-cell lysate as a control; 2, co-immunoprecipitates with anti-RagA; 3, co-immunoprecipitates with anti-RagB.

ACKNOWLEDGEMENTS

We thank E. K. Read (National Institute of Child Health and Human Development, National Institutes of Health, USA) for valuable advice and suggestions. This study was supported by Grants-in-Aid for Scientific Research (16791149 to the first author K. N., 15591957 to F. Y. and 15591958 to Y. M.) from the Japan Society for the Promotion of Science (JSPS) and the AGU High-Tech Research Centre Project from The Ministry of Education, Culture, Sports, Science and Technology, Japan. F. Y. was also supported partly by the Waksman Foundation in Japan.

REFERENCES

Andrés, M. T., Chung, W. O., Roberts, M. C. & Fierro, J. F. (1998). Antimicrobial susceptibilities of *Porphyromonas gingivalis*, *Prevotella intermedia*, and *Prevotella nigrescens* spp. isolated in Spain. *Antimicrob Agents Chemother* **42**, 3022–3023.

Bonass, W. A., Marsh, P. D., Percival, R. S., Aduse-Opoku, J., Hanley, S. A., Devine, D. A. & Curtis, M. A. (2000). Identification of *ragAB* as a temperature-regulated operon of *Porphyromonas gingivalis* W50 using differential display of randomly primed RNA. *Infect Immun* **68**, 4012–4017.

Bradburne, J. A., Godfrey, P., Choi, J. H. & Mathis, J. N. (1993). In vivo labeling of *Escherichia coli* cell envelope proteins with *N*-hydroxysuccinimide esters of biotin. *Appl Environ Microbiol* **59**, 663–669.

Curtis, M. A., Slaney, J. M., Carman, R. J. & Johnson, N. W. (1991). Identification of the major surface protein antigens of *Porphyromonas gingivalis* using IgG antibody reactivity of periodontal case–control serum. *Oral Microbiol Immunol* **6**, 321–326.

Curtis, M. A., Hanley, S. A. & Aduse-Opoku, J. (1999). The *rag* locus of *Porphyromonas gingivalis*: a novel pathogenicity island. *J Periodontal Res* **34**, 400–405.

Frandsen, E. V. G., Poulsen, K., Curtis, M. A. & Kilian, M. (2001). Evidence of recombination in *Porphyromonas gingivalis* and random distribution of putative virulence markers. *Infect Immun* **69**, 4479–4485.

Gardner, R. G., Russell, J. B., Wilson, D. B., Wang, G. R. & Shoemaker, N. B. (1996). Use of a modified *Bacteroides–Prevotella* shuttle vector to transfer a reconstructed β-1,4-D-endoglucanase gene into *Bacteroides uniformis* and *Prevotella ruminicola* B_14. *Appl Environ Microbiol* **62**, 196–202.

Grenier, D., Imbeault, S., Plamondon, P., Grenier, G., Nakayama, K. & Mayrand, D. (2001). Role of gingipains in growth of *Porphyromonas gingivalis* in the presence of human serum albumin. *Infect Immun* **69**, 5166–5172.

Hall, L. M. C., Fawell, S. C., Shi, X., Faray-Kele, M.-C., Aduse-Opoku, J., Whiley, R. A. & Curtis, M. A. (2005). Sequence diversity and antigenic variation at the *rag* locus of *Porphyromonas gingivalis*. *Infect Immun* **73**, 4253–4262.

Hamada, N., Sojar, H. T., Cho, M. I. & Genco, R. J. (1996). Isolation and characterization of a minor fimbria from *Porphyromonas gingivalis*. *Infect Immun* **64**, 4788–4794.

Hanley, S. A., Aduse-Opoku, J. & Curtis, M. A. (1999). A 55-kilodalton immunodominant antigen of *Porphyromonas gingivalis* W50 has arisen via horizontal gene transfer. *Infect Immun* **67**, 1157–1171.

Horton, R. M., Ho, S. N., Pullen, J. K., Hunt, H. D., Cai, Z. & Pease, L. R. (1993). Gene splicing by overlap extension. *Methods Enzymol* **217**, 270–279.

Ikeda, T. & Yoshimura, F. (2002). A resistance-nodulation-cell division family xenobiotic efflux pump in an obligate anaerobe, *Porphyromonas gingivalis*. *Antimicrob Agents Chemother* **46**, 3257–3260.

Imai, M., Murakami, Y., Nagano, K., Nakamura, H. & Yoshimura, F. (2005). Major outer membrane proteins from *Porphyromonas gingivalis*: strain variation, distribution, and clinical significance in periradicular lesions. *Eur J Oral Sci* **113**, 391–399.

Kamio, Y. & Nikaido, H. (1977). Outer membrane of *Salmonella typhimurium*. Identification of proteins exposed on cell surface. *Biochim Biophys Acta* **464**, 589–601.

Kleinfelder, J. W., Müller, R. F. & Lange, D. E. (1999). Antibiotic susceptibility of putative periodontal pathogens in advanced periodontitis patients. *J Clin Periodontol* **26**, 347–351.

Kumagai, Y., Konishi, K., Gomi, T., Yagishita, H., Yajima, A. & Yoshikawa, M. (2000). Enzymatic properties of dipeptidyl aminopeptidase IV produced by the periodontal pathogen *Porphyromonas gingivalis* and its participation in virulence. *Infect Immun* **68**, 716–724.

Lamont, R. J. & Jenkinson, H. F. (1998). Life below the gum line: pathogenic mechanisms of *Porphyromonas gingivalis*. *Microbiol Mol Biol Rev* **62**, 1244–1263.

Murakami, Y., Imai, M., Nakamura, H. & Yoshimura, F. (2002). Separation of the outer membrane and identification of major outer membrane proteins from *Porphyromonas gingivalis*. *Eur J Oral Sci* **110**, 157–162.

Murakami, Y., Imai, M., Mukai, Y., Ichihara, S., Nakamura, H. & Yoshimura, F. (2004). Effects of various culture environments on expression of major outer membrane proteins from *Porphyromonas gingivalis*. *FEMS Microbiol Lett* **230**, 159–165.

Nagano, K., Read, E. K., Murakami, Y., Masuda, T., Noguchi, T. & Yoshimura, F. (2005). Trimeric structure of major outer membrane

proteins homologous to OmpA in *Porphyromonas gingivalis*. *J Bacteriol* **187**, 902–911.

NCCLS (1997). *Methods for Antimicrobial Susceptibility Testing of Anaerobic Bacteria*, 5th edn, vol. 21. Approved standard M11-A5. Wayne, PA: National Committee for Clinical Laboratory Standards.

Nelson, K. E., Fleischmann, R. D., DeBoy, R. T., Paulsen, I. T., Fouts, D. E., Eisen, J. A., Daugherty, S. C., Dodson, R. J., Durkin, A. S. & other authors (2003). Complete genome sequence of the oral pathogenic bacterium *Porphyromonas gingivalis* strain W83. *J Bacteriol* **185**, 5591–5601.

Nishikawa, K. & Yoshimura, F. (2001). The response regulator FimR is essential for fimbrial production of the oral anaerobe *Porphyromonas gingivalis*. *Anaerobe* **7**, 255–262.

Ochman, H., Gerber, A. S. & Hartl, D. L. (1988). Genetic applications of an inverse polymerase chain reaction. *Genetics* **120**, 621–623.

Shi, X., Hanley, S. A., Faray-Kele, M. C., Fawell, S. C., Aduse-Opoku, J., Whiley, R. A., Curtis, M. A. & Hall, L. M. (2007). The *rag* locus of *Porphyromonas gingivalis* contributes to virulence in a murine model of soft tissue destruction. *Infect Immun* **75**, 2071–2074.

Thompson, J. D., Higgins, D. G. & Gibson, T. J. (1994). CLUSTAL W: improving the sensitivity of progressive multiple sequence alignment through sequence weighting, position-specific gap penalties and weight matrix choice. *Nucleic Acids Res* **22**, 4673–4680.

Yoshimura, F., Takahashi, K., Nodasaka, Y. & Suzuki, T. (1984). Purification and characterization of a novel type of fimbriae from the oral anaerobe *Bacteroides gingivalis*. *J Bacteriol* **160**, 949–957.